G-protein-mediated Interconversions of Cell-surface cAMP Receptors and Their Involvement in Excitation and Desensitization of Guanylate Cyclase in Dictyostelium discoideum

Haastert, Peter J.M. van; Wit, René J.W. de; Janssens, Pim M.W.; Kesbeke, Fanja; Goede, Jacob de

Published in:
Default journal

Publication date:
1986

THE JOURNAL OF BIOLOGICAL CHEMISTRY
© 1986 by The American Society of Biological Chemists, Inc.

Vol. 261, No. 15, Issue of May 25, pp. 6904–6911, 1986
Printed in U.S.A.

G-protein-mediated Interconversions of Cell-surface cAMP Receptors and Their Involvement in Excitation and Desensitization of Guanylate Cyclase in *Dictyostelium discoideum**

(Received for publication, April 29, 1985)

Peter J. M. van Haastert‡, René J. W. de Wit‡, Pim M. W. Janssens§, Fanja Kesbeke‡, and Jacob DeGoede¶

From the ‡Cell Biology and Morphogenesis Unit, Zoological Laboratory, and the ¶Department of Physiology and Physiological Physics, University of Leiden, 2300 RA Leiden and the §Laboratory of Biochemistry, University of Amsterdam, 1000 BH Amsterdam, The Netherlands

In *Dictyostelium discoideum* cells, extracellular cAMP induces the rapid (within 2 s) activation of guanylate cyclase, which is followed by complete desensitization after about 10 s. cAMP binding to these cells is heterogeneous, showing a subclass of fast dissociating sites coupled to adenylate cyclase (A-sites) and a subclass of slowly dissociating sites coupled to guanylate cyclase (B-sites). The kinetics of the B-sites were further investigated on a seconds time scale.

Statistical analysis of the association of [^{3}H]cAMP to the B-sites and dissociation of the complex revealed that the receptor can exist in three states which interconvert according to the following scheme.

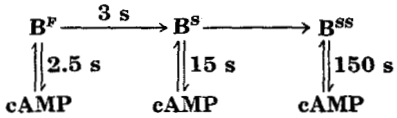

cAMP binds to the B^F-state (off-rate 2.5 s) which rapidly ($t_{½}$ = 3 s) converts to the B^S-state (off-rate 15 s) and subsequently (without a detectable delay) into the B^{SS}-state (off-rate 150 s). In membranes, both the B^S- and B^{SS}-states are converted to the B^F-state by GTP and GDP, suggesting the involvement of a G-protein.

Desensitized cells show a 80% reduction of the formation of the B^{SS}-state, but no reduction of the B^F- or B^S-state.

These data are combined into a model in which the transitions of the B-sites are mediated by a G-protein; activation of the G-protein and guanylate cyclase is associated with the transition of the B^S- to the B^{SS}-state of the receptor, whereas desensitization is associated with the inhibition of this transition.

The eukaryotic microorganism *Dictyostelium discoideum* is a suitable organism to study signal transduction. In this organism, the hormone-like substance is cAMP which is detected by cell-surface receptors. Extracellular cAMP induces the rapid activation of guanylate cyclase (1) and the slower activation of adenylate cyclase (2). Intracellular cGMP reaches a peak after 10 s, declines to prestimulated levels reached at about 30 s (3), and is supposed to be involved in the cAMP-induced chemotactic reaction (4). Intracellular cAMP reaches maximal levels after 60–120 s and is secreted, thus acting as an autocatalytic feedback loop (5).

Prolonged stimulation of *D. discoideum* cells with constant cAMP concentrations induces desensitization by at least two mechanisms: (i) down-regulation of cAMP binding activity after a long incubation (5–30 min) with high cAMP concentrations (1–100 μM) (after removal of cAMP, cells resensitize with a half-life of about 60 min (6, 7)); (ii) a rapid desensitization of the cAMP-mediated activation of the cyclases by nanomolar cAMP concentrations (8, 9) without a loss of cAMP-binding sites (after removal of cAMP, cells resensitize with a half-life of 1–2 min for the guanylate cyclase (9) and 3–4 min for the adenylate cyclase (10)). Desensitization of the cAMP-mediated cGMP accumulation is completed within about 10 s (9), whereas desensitization of the cAMP accumulation is completed only after about 5 min (11). The mechanism of excitation and desensitization of the cGMP response is the subject of the present report.

A second chemotactic compound in *D. discoideum* is folate (12). Binding of cAMP or folate to sensitive cells is heterogeneous in respect to kinetic properties (13–15). Since binding of both compounds shows essentially identical complexity, we will unify the previously used notations for the different forms of the receptor. The major portion (~96%) of binding sites are fast dissociating ($t_{½}$ = 1–2 s) and are designated as A-sites. The A-sites may exist in two states, A^H and A^L, with high and low affinity, respectively. cAMP induces a time- and concentration-dependent transition of A^H to A^L, a transition which can be induced in membranes by guanine nucleotides, suggesting the involvement of a guanine nucleotide regulatory protein (G-protein) in this transition (16, 17). The A-sites appear to be responsible for the activation of adenylate cyclase in *D. discoideum* (18–20).

A second class of binding sites releases bound cAMP more slowly. This class of binding sites is designated B-sites and may exist in at least two states, B^S and B^{SS}, which have a half-life of dissociation equal to 15 and 150 s, respectively (13–15). The B-sites are also sensitive to guanine nucleotides (16, 21) and are most likely involved in the activation of guanylate cyclase (18, 20).

We have analyzed the kinetics of the B-sites in more detail and present evidence for a cAMP-induced interconversion between three states of the receptor that are related to the interaction of receptor with a G-protein. Cells subjected to homologous desensitization of guanylate cyclase (22) show a strongly reduced binding to only one of these states, whereas

* This work was supported by the Foundation for Fundamental Biological Research (Biologisch Onderzoek Nederland) and the C. and C. Huygens Fund, which are subsidized by the Netherlands Organization for the Advancement of Pure Scientific Research (Zuiver Wetenschappelijk Onderzoek). The costs of publication of this article were defrayed in part by the payment of page charges. This article must therefore be hereby marked "*advertisement*" in accordance with 18 U.S.C. Section 1734 solely to indicate this fact.

binding to the others is not altered. A model on the interaction between B-sites and G-protein is presented.

EXPERIMENTAL PROCEDURES

Materials—[2,8-^{3}H]cAMP (1.5 TBq/mmol) was obtained from The Radiochemical Centre, Amersham, United Kingdom. cAMP, GTP, GDP, GMP, and dithiothreitol were from Sigma, GppNHp,[1] ATP, ADP, and AppNHp were purchased from Boehringer Mannheim. GTPγS was a generous gift of Dr. F. Eckstein (Max-Planck-Institut fur experimentelle Medizin, Göttingen, West Germany). Silicon oils (AR 20 and AR 200) were obtained from Wacker Chemie.

Culture Conditions—D. discoideum NC-4(H) cells were grown with *Escherichia coli* 281 on a solid medium containing 3.3 g of peptone, 3.3 g of glucose, 4.5 g of KH_2PO_4, 1.5 g of $Na_2HPO_4 \cdot 2H_2O$, and 15 g of agar/liter. Cells were harvested in the late logarithmic phase with 10 mM sodium/potassium phosphate buffer, pH 6.5 (Pb buffer), and freed from bacteria by repeated centrifugations at 100 × *g* for 4 min.

Preparation of Membranes (23)—Cells were starved for 4.5 h by shaking in Pb buffer, centrifuged, washed twice, and resuspended in this buffer at 2×10^8 cells/ml. Air was bubbled through the suspension for about 10 min at 20 °C. The cells were then transferred to 0 °C and broken by passage through a Nucleopore filter (diameter, 25 mm; pore size, 3 μm). The filter was washed with an equal volume of Pb buffer, and the combined homogenates were centrifuged at 10,000 × *g* for 5 min at 0 °C. The supernatant was removed, and the pellet was resuspended in Pb buffer at a concentration equivalent to 1.25×10^8 cells/ml. Membranes were kept on ice during the entire experiment, which did not last longer than 1 h.

cAMP Binding Assays (13)—All binding experiments have been performed at 20 °C except when indicated. The incubation mixture was in a total volume of 100 μl of Pb buffer with 5 mM dithiothreitol (an inhibitor of phosphodiesterase in *D. discoideum* (24)), different concentrations of [^{3}H]cAMP, and 10^7 cells or membranes derived from 10^7 cells. Binding of cAMP to all sites was measured by centrifugation of 95 μl of the incubation mixture through silicon oil (AR 200:AR 20 = 1:2). Binding to the slowly dissociating sites was measured by a squirt of 1 ml of Pb buffer with 0.1 mM cAMP and 5 mM dithiothreitol into the incubation mixture, followed by centrifugation of 1 ml of the mixture through silicon oil. Cells were centrifuged for 15 s, and membranes for 30 s. The efficiency of the centrifugation step was investigated by measuring the protein content of the pellet. The amount of protein was recovered quantitatively in the pellet below the silicon oil when concentrated cells, 11-fold diluted cells, or concentrated membranes were used. However, when 10-fold diluted membranes (equivalent to 10^7 cells/ml) are centrifuged, only 25% of the protein is recovered in the pellet after a 30-s centrifugation period. Therefore, binding experiments with membranes have been performed only with concentrated membrane preparations.

Identification of Cell-associated Radioactivity—Tubes contained 10 μl of 20% (w/v) sucrose in 3.5% (v/v) perchloric acid and 200 μl of silicon oil. Cells were incubated with 10 nM [^{3}H]cAMP as described above and were centrifuged through silicon oil at the moment of binding equilibrium, at 10 s, or at 2 min after the onset of dissociation. The tip of the tubes containing the cell-associated radioactivity was cut, and the content of four tips was added to 200 μl of Pb buffer. The lysate was neutralized with 20 μl of $KHCO_3$ (50% saturated at 20 °C) and centrifuged at 10,000 × *g* for 2 min, and the supernatant was analyzed by high pressure liquid chromatography (25). The column was LiChrosorp RP-18; the mobile phase was 25 mM tributylammonium formate, 15% methanol, pH 3.0; the flow rate was 1 ml/min. The retention times of cAMP and its derivatives are: dead time, 2.5 min; adenosine, 3.24 min; 5′-AMP, 4.58 min; cIMP, 5.18 min; cAMP, 8.31 min. At least 95% of the radioactivity bound to cells at equilibrium, at 10 s, or at 2 min after dissociation co-eluted with authentic cAMP.

Data Analysis of the Release of Bound [^{3}H]cAMP—Cells or membranes were incubated with [^{3}H]cAMP until equilibrium. The release of bound [^{3}H]cAMP was initiated by the addition of excess cAMP or by dilution of the incubation mixture. The residual [^{3}H]cAMP bound was measured at time t_i, with n_i as the number of replicas and N as the number of time points.

The release of bound [^{3}H]cAMP as a function of time was fitted to sums-of-exponentials models.

$$y(t) = \sum_{j=1}^{a} A_j e^{-\alpha j t} \qquad a = 1, 2, 3, 4 \tag{1}$$

To this end, the mean (z_i) of the replicas at time t_i was used as the single value, and the sample variance (σ_i^2) of the replicas was divided by their number n_i as weights. To find the optimal parameter set, the minimum of the weighted residual sum of squares (WRSS) at the N time points (26) was searched.

$$\mathrm{WRSS} = \sum_{i=1}^{N} (Z(t_i) - y(t_i))^2 \frac{n_i}{\sigma_i^{-2}} \tag{2}$$

The minimum was found by using a nonlinear Marquardt-type minimalization procedure.

To estimate the model order (26, 27) (*i.e.* the number of exponentials in Equation 1), we determined the minimum value of the Akaike information criterion (AIC),

$$\mathrm{AIC} = \mathrm{WRSS} + 2p \tag{3}$$

in which p is the number of free parameters in the model. The order of the model was also estimated by using the F test (26, 27),

$$\mathrm{F} = \frac{N - p_2}{p_2 - p_1} \frac{\mathrm{WRSS}_1 - \mathrm{WRSS}_2}{\mathrm{WRSS}_2} \tag{4}$$

where the subscripts 1 and 2 denote the smaller and larger model, respectively. The degrees of freedom of F are ($p_2 - p_1$, $N - p_2$).

RESULTS

Kinetics of the Release of Bound [^{3}H]cAMP Demonstrate Three Components—Cells were incubated with 2 nM [^{3}H]cAMP until equilibrium. Dissociation of bound [^{3}H]cAMP was initiated either by the addition of excess cAMP, as we did previously (13), or by the addition of excess cAMP with an 11-fold dilution of the incubation mixture. A semilogarithmic plot is presented in Fig. 1. Apparently, both methods of dissociation yield the same result. However, addition of excess cAMP in combination with an 11-fold dilution has the advantage that nonspecific binding is reduced 11-fold. Therefore, it becomes possible to follow the release of bound [^{3}H]cAMP for a longer period. The results suggest the presence of a very slowly dissociating site with $t_{½}$ of about 2 min, which we designate as B^{SS}.

The semilogarithmic plot of Fig. 1 clearly shows that dissociation is multiphasic. The data were fitted to two, three, and four exponential models, and a decision for the best fit was made with the AIC test and with the F test (see "Experimental Procedures"). The fit with the lowest AIC value yields the optimal number of exponentials involved in the dissociation process.

The experiment presented in Fig. 1 is best described by the sum of three exponentials. The results indicate that 69% of the bound [^{3}H]cAMP dissociates with $k_{-1} = 0.47\ s^{-1}$, 21% with $k_{-1} = 0.042\ s^{-1}$, and 10% with $k_{-1} = 0.005\ s^{-1}$.

Next we wish to establish whether these three exponentials must relate to three receptor forms or if two forms (X and Y) with interconversions during the dissociation can also explain the result. The mathematical description of such a model leads to only two exponentials, indicating that at least three receptor forms are observed in dissociation experiments. These three forms are designated as Fast, B^S, and B^{SS} according to previous nomenclature (13–15). It should be noticed that Fast is a mixture of multiple forms with similar k_{-1}, notably A^H and A^L (13), and B^F (this report).

[1] The abbreviations used are: GppNHp, guanyl-5′-yl imidodiphosphate; GTPγS, guanosine 5′-*O*-(3-thiotriphosphate); AppNHp, adenyl-5′-yl imidodiphosphate; AIC, Akaike information criterion.

[2] It should be noted that cAMP does accelerate the release of bound [^{3}H]cAMP when cells (or membranes prepared from them) were used which were starved in suspension for an unphysiologically long period (7–9 h). Cells starved on a solid support for the same period do not show this effect.

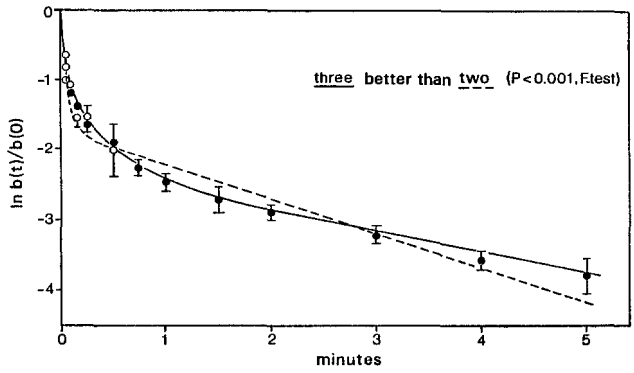

FIG. 1. **Semilogarithmic plot of the release of bound [^{3}H]cAMP from cells.** *D. discoideum* cells were equilibrated with 2 nM [^{3}H]cAMP at 20 °C for 45 s in a total volume of 100 μl. At $t = 0$ s, either 2 μl of 10 mM cAMP was added and 95 μl of the incubation mixture was centrifuged through silicon oil at the times indicated (○) or 1 ml of buffer with 0.1 mM cAMP was added and 1 ml of the mixture was centrifuged at the times indicated (●). $b(t)$ is the specific binding at t min after the onset of dissociation. $b(0)$ stands for the specific binding at $t = 0$ s and was 1275 ± 51 dpm/10^7 cells. Nonspecific binding was measured by including 0.1 mM cAMP in the preincubation mixture and was determined as 153 ± 8 dpm/10^7 cells (○) and 16 ± 1 dpm/10^7 cells (●). The results shown are the means and standard deviations of the logarithm of quadruplicate determinations of a typical experiment reproduced four times. The data were subjected to weighted, least squares curve fitting using the sum of two, three, or four exponentials (see "Experimental Procedures"). Statistical analysis indicates that the curve is described better (lower AIC values) by the sum of three exponentials than by the sum of two or four exponentials: AIC = 119 for two exponentials, AIC = 19.5 for three exponentials, and AIC = 22.3 for four exponentials. The same conclusion is reached when an F test is used. The values of the parameters for the three exponentials are mentioned in the text.

Finally, we would like to establish whether these forms interconvert during the dissociation experiment or whether they dissociate independently of each other. Unfortunately, discrimination between these possibilities is not possible from single dissociation experiments.

Dissociation of Bound [^{3}H]cAMP at Different Conditions—The conditions include dissociation of [^{3}H]cAMP bound to cells after equilibration with different concentrations of radioligand, dissociation in the absence or presence of free cAMP, and dissociation of [^{3}H]cAMP bound to membranes (Table I). The statistical analysis (AIC values) reveals that at all conditions the dissociation curves are best described by three components. The F test at the level of significance of 0.05 leads to the same model order.

The apparent off-rates of B^S and B^{SS} are not statistically different when cells are equilibrated with 2, 10, 30, or 100 nM [^{3}H]cAMP. Furthermore, essentially the same off-rates were observed for the dissociation of [^{3}H]cAMP that was bound to membranes. In the previous experiments, dissociation of [^{3}H]cAMP was observed while all receptors were occupied with [^{3}H]cAMP or cAMP. The detection of the dissociation kinetics while only a small minority of the receptors are occupied requires the equilibration of cells with a low concentration of [^{3}H]cAMP (*e.g.* only 2% of the receptors are occupied at 2 nM cAMP). Dissociation is induced by dilution of the incubation mixture, which prevents reassociation of [^{3}H]cAMP. This experiment cannot be performed at 20 °C because cells start to secrete cAMP at about 60–90 s after addition of [^{3}H]cAMP (8, 13, 28, 29). However, this secretion is delayed until at least 5 min if the temperature is reduced to 0 °C (29). Thus, cells were equilibrated at 0 °C with 2 nM [^{3}H]cAMP, which was followed by an 11-fold dilution of the incubation mixture with buffer or with buffer and excess cAMP. The results (Table I) reveal no statistically relevant difference between these two methods. The reduction of the off-rates at 0 °C compared to 20 °C is most likely due to the lowered temperature.[2]

The statistical analyses of the exponential curve fitting of the dissociation of bound [^{3}H]cAMP (Table I) can be summarized as follows. Under all conditions, we observed three forms, Fast, B^S, and B^{SS}. Their rate constant of dissociation was not affected by the condition used. If these three forms would interconvert during the process of dissociation, then these interconversions are not affected by the concentration of [^{3}H]cAMP present during equilibration, the concentration of free cAMP present during dissociation, nor a cytosolic component (*e.g.* ATP).

Number and Affinity of B^S and B^{SS}—Table I contains the results of dissociation experiments in which cells were equilibrated at 20 °C with different concentrations of [^{3}H]cAMP. The number of binding sites that were occupied with [^{3}H]cAMP at the onset of dissociation was obtained for the three components, Fast, B^S, and B^{SS}. These binding data are presented in Fig. 2 as a Scatchard plot (*open symbols*).

Since we observed no interconversions of the three forms during the course of the dissociation, it should be possible to calculate the occupancy of Fast, B^S, and B^{SS} at equilibrium by a more simple procedure. The rate constants of dissociation (k_{-1}) are known from Table I for cells at 20 °C: Fast, k_{-1} = 0.43–0.73 s^{-1}; B^S, $k_{-1} = (4.3 \pm 0.4) \times 10^{-2}$ s^{-1}; B^{SS}, $k_{-1} = (4.75 \pm 0.4) \times 10^{-3}$ s^{-1}. Therefore, it can be calculated that binding of [^{3}H]cAMP to Fast is lost after a dissociation period of 10 s, whereas binding of B^S is reduced to 65.1 ± 2.8% and binding of B^{SS} is reduced to 95.4 ± 0.4%. After a dissociation period of 120 s, binding to both Fast and B^S has been lost; binding to B^{SS} is reduced to 55.6 ± 2.7%.

This is described by the following set of equations

$$b(0) = \text{Fast}(0) + B^S(0) + B^{SS}(0) \quad (5a)$$

$$b(10) = (0.651 \pm 0.028)\ B^S(0) + (0.954 \pm 0.0004)\ B^{SS}(0) \quad (5b)$$

$$b(120) = (0.556 \pm 0.027)\ B^{SS}(0) \quad (5c)$$

Thus, by observing the binding at equilibrium, $b(0)$, and at 10 and 120 s after the onset of dissociation, it is possible to calculate the occupancy of the three components at equilibrium (Fast(0), $B^S(0)$, and $B^{SS}(0)$).

This "back-calculation" was done for experiments using different concentrations of [^{3}H]cAMP. The results are also presented in the Scatchard plot of Fig. 2 (*closed symbols*). We emphasize that the data points obtained by experimental curve fitting and by back-calculation lie close together. This further supports the validity of the back-calculation. A cell contains about 77,000 fast dissociating sites; the curve is convex upward, in agreement with previous observations (13) that this class is composed of high affinity (A^H, K_d = 60 nM) and low affinity (A^L, K_d = 450 nM) sites. In addition, a cell contains about 2300 B^S-sites and about 1100 B^{SS}-sites; curves are approximately linear, yielding an apparent K_d of 13 nM for both receptor forms.

In this and the previous sections, we did not find any evidence for a transition among the B-sites during their dissociation. When these transitions are absent, it is possible to calculate the occupancy of B^S and B^{SS} at the onset of dissociation by differential dissociation using Equation 5 (a–c). This method is preferred above exponential curve fitting because it is less time-consuming and requires at least 5-fold less data points than exponential curve fitting to obtain the same accuracy.

Kinetics of Association of [^{3}H]cAMP to B^S and B^{SS}—In the

TABLE I

Statistical analysis of the release of bound [^{3}H]cAMP under different conditions

Condition[a]	AIC values[b]			Fitted parameters for $a = 3$[c]					
				k_{-1}			Occupied sites/cells		
	$a = 2$	$a = 3$	$a = 4$	Fast	B^S	B^{SS}	Fast	B^S	B^{SS}
				$s^{-1} \times 10$	$s^{-1} \times 100$	$s^{-1} \times 1{,}000$			
Cells									
2 nM (15, 7)	103	17.4	19.6	4.7 ± 0.3	4.2 ± 0.7	4.9 ± 0.4	955 ± 36	300 ± 25	143 ± 13
10 nM (15, 5)	114	14.8	18.8	5.8 ± 0.3	4.2 ± 0.4	4.8 ± 0.3	3,880 ± 66	980 ± 52	460 ± 35
30 nM (15, 5)	128	17.3	21.0	6.6 ± 0.2	4.1 ± 0.6	4.6 ± 0.5	8,720 ± 167	1,600 ± 107	750 ± 82
100 nM (15, 5)	167	15.3	18.1	7.3 ± 0.3	4.7 ± 0.5	4.7 ± 0.5	20,600 ± 400	1,910 ± 70	910 ± 64
Membranes (16, 7)	84	26.5	32.5	3.6 ± 0.4	4.3 ± 0.6	3.9 ± 0.9	2,380 ± 130	1,060 ± 110	275 ± 45
Cells, 0 °C									
Chase (16, 4)	277	43.5	47.4	2.1 ± 0.4	3.1 ± 0.5	1.7 ± 0.6	837 ± 72	440 ± 61	73 ± 14
Dilution (14, 4)	86	29.1	35.0	2.1 ± 0.3	2.8 ± 0.5	1.8 ± 1.1	848 ± 62	424 ± 49	79 ± 23

[a] Unless specified, the experiments were performed at 20 °C, dissociation was started by excess cAMP, and the concentration of [^{3}H]cAMP was 2 nM. The values in parentheses indicate the number of time points and the number of replicas at these time points, respectively; their multiplication yields the total number of data points used for the fit.

[b] The experimental data were fitted by using the sum of two, three, or four exponentials (indicated by a values). AIC values were calculated with Equation 3; their lowest value yields the preferred model (see "Experimental Procedures").

[c] Values are the means and standard deviations.

previous section, it was shown that the different forms probably do not interconvert during dissociation. Michaelis-Menten kinetics should be applicable if they also do not interconvert during association. The following equations should then be valid

$$b(t) = b(\infty)(1 - e^{-k_{on} \cdot t}) \quad (6a)$$

or

$$-\ln(1 - b(t)/b(\infty)) = k_{on} \cdot t \quad (6b)$$

where

$$k_{on} = k_1[\text{cAMP}] + k_{-1} \quad (6c)$$

In these Equations, $b(t)$ is cAMP bound at time t, $b(\infty)$ is cAMP bound at equilibrium, and k_{on} is the apparent on-rate.

Thus, the association of [^{3}H]cAMP to B^S and B^{SS} was determined (Fig. 3, *A* and *B*). The data were replotted according to Equation 6b, yielding a slope equal to the apparent on-rate, k_{on} (Fig. 3*C*). The k_{on} was determined for different concentrations of [^{3}H]cAMP. Finally, the k_{on} was presented against the concentration of [^{3}H]cAMP (Fig. 3*D*), which should yield a straight line when Michaelis-Menten kinetics are applicable (Equation 6c). The apparent k_{-1} of B^S and B^{SS} and their apparent K_d are known from Table I and Fig. 2. The predicted curve for B^S and B^{SS} is quite different from observed kinetics. Thus, we must reject the hypothesis that association follows Michaelis-Menten kinetics.

First, cAMP associates to B^{SS} about 10-fold faster than predicted using known values of k_{-1} and K_d. At 2 nM [^{3}H]cAMP, the half-time of association should be about 150 s; however, equilibrium is reached within 60 s, and half-maximal occupancy is obtained after about 10 s. This suggests that the occupied B^{SS}-form does not arise from association of cAMP to the empty B^{SS}-site, but by the conversion of another occupied site which associates with faster kinetics. Second, association of [^{3}H]cAMP to B^S and B^{SS} at high [cAMP] is independent of the cAMP concentration. Apparently, association of cAMP to B^S and B^{SS} cannot exceed an apparent k_{on} of 0.22 s^{-1}. This implies that also the occupied B^S-form arises from a conversion of a form with faster association kinetics and that the rate of conversion is 0.22 s^{-1}.

These results may suggest the following scheme of interactions during association of cAMP to the B-sites (see also "Discussion"). Initially, cAMP binds to a fast dissociating form; subsequently this site converts into B^S. This conversion shows a half-life of 3 s ($k = 0.22$ s^{-1}). Finally, B^S converts to B^{SS} without a detectable delay.

Binding of [^{3}H]cAMP to Desensitized Cells—cAMP induces the rapid desensitization of guanylate cyclase, which is completed after about 10–20 s (9). Fig. 4 presents the binding of 2 nM [^{3}H]cAMP to the Fast, B^S, and B^{SS} forms at two conditions: either 2 nM cAMP and 2 nM [^{3}H]cAMP were added simultaneously (*closed symbols*) or cells were desensitized by 2 nM cAMP given at $t = 0$ s and binding was measured with 2 nM [^{3}H]cAMP given at $t = 20$ s (*open symbols*). Thus, the binding of 2 nM [^{3}H]cAMP to regular and desensitized cells was measured. Fig. 4 shows that binding of [^{3}H]cAMP to Fast and B^S in control and desensitized cells is essentially the same. In contrast, binding to B^{SS} is reduced about 80% upon the preincubation with cAMP.

Guanine Nucleotides Modulate B^S and B^{SS} in Membranes—Previously, we have demonstrated that guanine nucleotides interfere with cAMP binding to membranes from *D. discoideum* (16, 21); the number of B^S and B^{SS}-sites was reduced by GTP or GDP, whereas the total number of binding sites was not altered.

The experiment presented in Fig. 5 was set up to test whether both B^S and B^{SS} are sensitive to guanine nucleotides and especially to test to which form they interconvert upon addition of guanine nucleotides. Membranes were incubated with [^{3}H]cAMP until equilibrium was reached. Then, at $t =$ 0 s, excess cAMP was added, and GTP or GDP was added at 10 or 120 s. The results were analyzed by computer-assisted curve fitting (Table II).

Membranes possess three binding forms which dissociate with similar rate constants if compared to cells. Their proportioning at 2 nM [^{3}H]cAMP is 65% Fast, 29% B^S, and 7% B^{SS}. When only the data points at 10 s and later are taken into account, further dissociation should be described by only two components, B^S and B^{SS}, because all Fast sites have dissociated. The distribution of residual bound [^{3}H]cAMP at $t = 10$ s is 0 Fast, 20% B^S, and 7% B^{SS}. When GDP or GTP

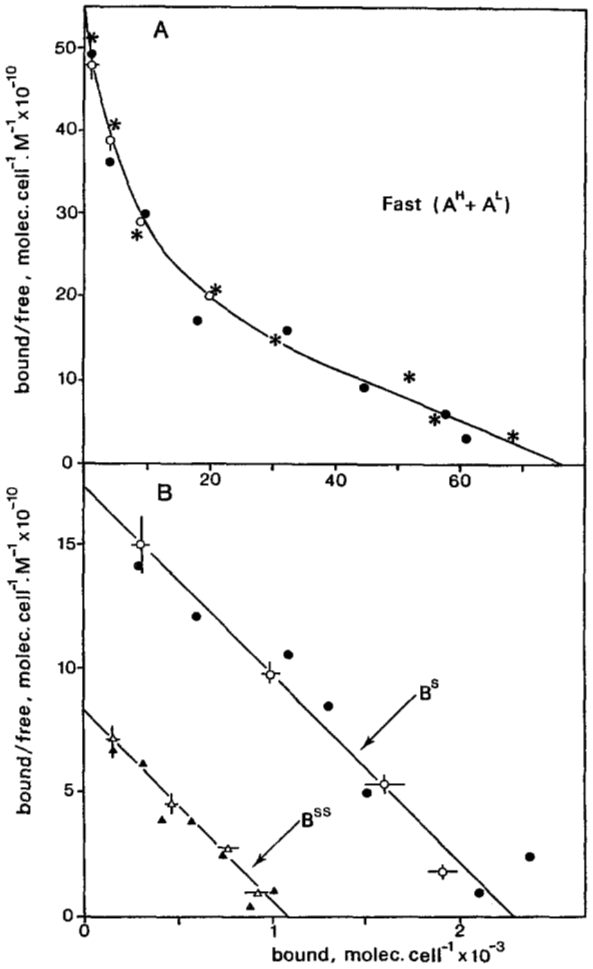

FIG. 2. **Scatchard plots of fast dissociating sites and B^S and B^{SS}.** This figure consists of data obtained from exponential curve fitting in Table I (○, △) and data obtained by back-calculation (●, ▲). For the latter method, cells were incubated with different concentrations of [^{3}H]cAMP (2–2000 nM) for 45 s. Then cells were centrifuged through silicon oil directly (yielding $b(0)$) or at 10 or 120 s after addition of excess cAMP (yielding $b(10)$ and $b(120)$, respectively). Binding to Fast, B^S, and B^{SS} at equilibrium was calculated using Equation 5 (a–c). The results of three experiments with triplicate incubations were combined. The data on Fast that were published previously (Fig. 6 of Ref. 13) are indicated by the *asterisks*.

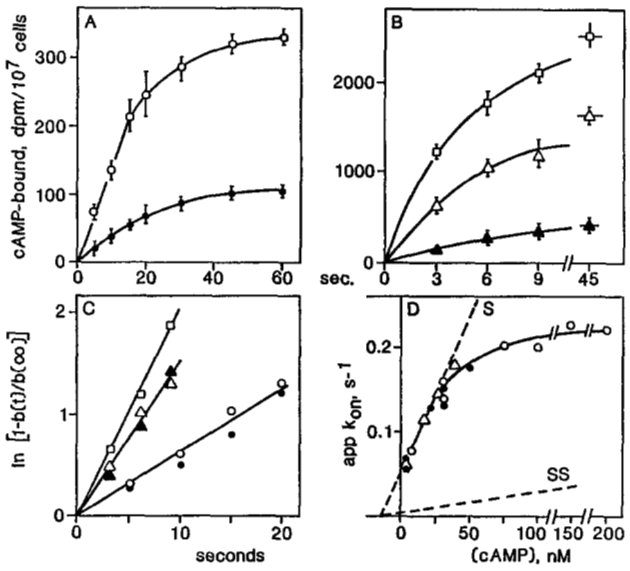

FIG. 3. **Kinetics of association of [^{3}H]cAMP to B^S and B^{SS}.** Cells were incubated with [^{3}H]cAMP for the times indicated in *A–C* in a volume of 100 μl. Then 1 ml of buffer with 0.1 mM cAMP was added, and 1 ml of the mixture was layered on top of silicon oil. Tubes were centrifuged at 10 s (*open symbols*) or at 2 min (*closed symbols*) after the cAMP chase. *A* and *B*, the cAMP concentrations used were 2 nM (*A*: ○, ●), 30 nM (*B*: △, ▲), and 100 nM (*B*: □). Data are the means and standard deviations of quadruplicate incubations. Nonspecific binding, which is subtracted from all data, was 11.1 ± 0.6 dpm (○, ●), 165 ± 6 dpm (△, ▲), and 491 ± 15 dpm (□), all with $n = 6$. *C*, replot of the data of *A* and *B*, where $b(t)$ is the binding at time t and $b(\infty)$ is the binding at equilibrium (45–60 s). *D*, association kinetics were measured at different [^{3}H]cAMP concentrations as shown in *A* and *B*. The slope in the logarithmic plot (*C*) equals the apparent k_{on} ○, k_{on} of B^S + B^{SS} (10-s dissociation); ●, k_{on} of B^{SS} (2-min dissociation); △, 8-s chase (data from Ref. 13). The theoretical curves for B^S and B^{SS} (*dashed lines*) are based on the observed dissociation constants (Fig. 2) and off-rate (k_{-1}, Table I).

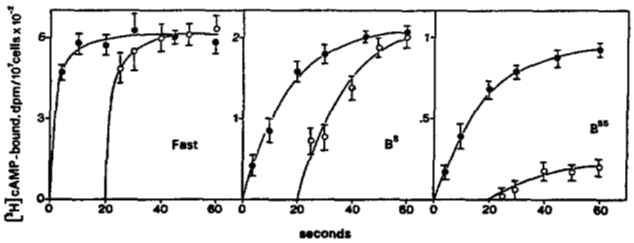

FIG. 4. **Binding of [^{3}H]cAMP to desensitized cells.** The incubation mixture was composed 2 × 10^8 cells in 180 μl, 20 μl of 20 nM cAMP, and 200 μl of 2 nM [^{3}H]cAMP. For control cells (●), all components were mixed simultaneously at $t = 0$; for desensitized cells (○), cells and cAMP were mixed at $t = 0$, and [^{3}H]cAMP was added at $t = 20$ s. Thus, the concentration of cyclic nucleotide remained 2 nM during the entire experiment. At the times indicated binding of [^{3}H]cAMP was measured directly or at 10 or 120 s after a chase with excess cAMP. Binding to the Fast-, B^S- and B^{SS}-sites was calculated using Equation 5 (a–c). Nonspecific binding has been subtracted from the data. Shown are the means and standard deviations of quadruplicate determinations reproduced three times.

is added at 10 s, the dissociation is optimally described again by three components: 19% Fast with $k_{-1} = 0.3$ s^{-1}, 5% B^S, and 3% B^{SS}. This suggests that the majority of B^S is transferred by GTP or GDP to a fast dissociating form. B^{SS} is also affected by guanine nucleotides, but a decision about its transfer to B^S or Fast cannot yet be made. The distribution of bound [^{3}H]cAMP at 2 min after the onset of dissociation is 0 Fast, 0 B^S, and 5% B^{SS}. The addition of GTP or GDP at this moment results in the enhanced release of bound [^{3}H]cAMP. The analysis indicates only two components: 3% Fast with k_{-1} = 0.21 s^{-1} and 2% B^{SS}. B^S is not present, indicating that also the B^{SS} is transferred to a fast dissociating site by guanine nucleotides. It should be noticed that GTP and GDP and the nonhydrolyzable analog GTPγS (data not shown) have similar effects.

Specificity of Guanyl Nucleotides—Membranes were incubated with 2 nM [^{3}H]cAMP in the presence of nucleotides until equilibrium, which is followed by a 10-s dissociation with excess cAMP (Fig. 6). Guanyl nucleotides inhibit the thus measured cAMP binding by maximally 80%. A half-maximal effect is observed at about 2.5 μM GTP, GDP, and GTPγS and at about 16 μM GppNHp; GMP is about 1000-fold less active than GTP. This specificity is consistent with the action of a guanine nucleotide regulatory protein (G-protein). Interestingly, ATP strongly stimulates cAMP binding measured at 10 s after a cAMP chase; ADP is without effect, and AppNHp slightly inhibits cAMP binding. Recent results suggest that this effect of ATP is mediated by protein kinase C (30).

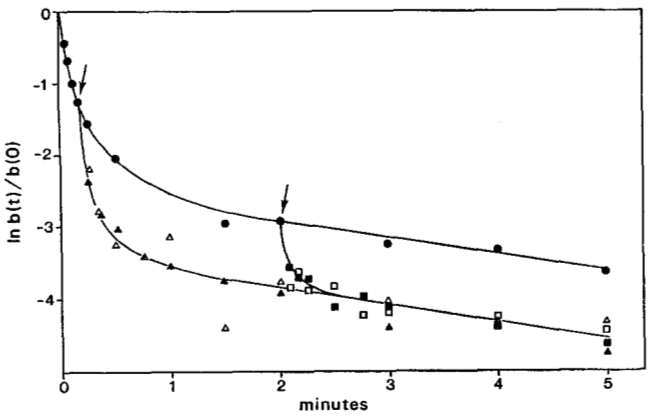

FIG. 5. **Effect of GTP and GDP on the dissociation of the [^{3}H]cAMP-receptor complex in membranes.** Membranes of *D. discoideum* cells were prepared by shearing the cells through a Nucleopore filter (see "Experimental Procedures") and were preincubated at 20 °C with 2 nM [^{3}H]cAMP in a total volume of 100 μl for 75 s. Then, at $t = 0$, 2 μl of 10 mM cAMP was added and membranes were centrifuged through silicon oil at the times indicated. At the times indicated by the *arrows*, 5 μl of GTP or GDP (0.1 mM final concentration) was added. ●, control; ▲, GTP added at 10 s; △, GDP, added at 10 s; ■, GTP added at 2 min; □, GDP added at 2 min. Nonspecific binding was 185 ± 8 dpm/incubation, and specific binding at $t = 0$ s was 3185 ± 102 dpm/incubation. The data shown are the means of triplicate determinations from an experiment reproduced two times. The combined data were subjected to computer-assisted curve fitting and statistical analysis (see Table II).

DISCUSSION

Binding of cAMP to *D. discoideum* cells is a complex phenomenon. Previously, we observed a class of fast dissociating sites (A-sites with $t_{½} = 1$–2 s) that are guanine nucleotide-sensitive and that are presumably responsible for the activation of adenylate cyclase by extracellular cAMP. A second class of binding sites is slowly dissociating (B-sites with $t_{½} = 15$–150 s); these sites are also sensitive to guanine nucleotides and are probably involved in the activation of guanylate cyclase in this organism (13–21). In this study, we further analyzed the kinetics of the B-sites. The major findings are the following. 1) Computer-assisted analysis of the release of bound [^{3}H]cAMP indicates that the dissociation should be described by three components rather than by two or four. These forms are called Fast, B^S, and B^{SS}. 2) No interconversions between these forms were observed during the process of dissociation that were induced by cAMP or by a cytosolic regulator. 3) In contrast, association of [^{3}H]cAMP to B^S and B^{SS} does not follow simple Michaelis-Menten kinetics; occupied B^S and B^{SS} sites are formed from a transition of a faster dissociating form. 4) Cells whose guanylate cyclase is desensitized by preincubation with cAMP for 20 s show a strongly reduced binding of [^{3}H]cAMP to B^{SS}, but no reduction to the Fast and B^S form. 5) Guanine nucleotides transfer the majority of B^S and B^{SS} to a form which dissociates much faster. These results strongly suggest that the transitions between the different states of the B-sites are mediated by a G-protein and may relate to the activation and desensitization of guanylate cyclase in *D. discoideum*.

The interaction of hormone receptors, G-protein, guanine nucleotides, and adenylate cyclase in vertebrates has been studied in great detail (31–33), resulting in the general scheme presented in Fig. 7A. Four G-protein-receptor components are arranged in a cycle: LR, LRN·GDP, LRN, and LRN·GTP, where L is the ligand, R is the receptor, and N is the G-protein. The ligand binds to the receptor, yielding LR, which couples to N·GDP. The complex is unstable, and GDP is replaced by GTP. The G-protein is activated (N·GTP) and interacts with adenylate cyclase, resulting in enhanced activity. The G-protein is a GTPase; hydrolysis of GTP results in the deactivation of adenylate cyclase. The G-protein is a heterotrimer composed of an α-subunit which possesses the guanine nucleotide-binding site and GTPase activity, a β-subunit which regulates the activity of the α-subunit, and a γ-subunit with unknown function (34–36). Dissociation of the heterotrimer has been observed during its activation by GTP (37–39).

We adopt this basic scheme to interpret our previous observations on the receptor class coupled to adenylate cyclase (A-sites) and the present observations on the receptor class coupled to guanylate cyclase (B-sites).

The cAMP receptor that is coupled to adenylate cyclase in *D. discoideum* (A-sites) can exist in two distinguishable states: A^H with high affinity for cAMP and A^L with low affinity (13). cAMP binding to membranes shows high affinity in the absence and low affinity in the presence of GTP or GDP (16). This indicates that LRN·GTP and LRN·GDP are represented by the low affinity state (Fig. 7*B*). Binding of cAMP to intact cells starts with the high affinity state, A^H, which converts to the low affinity state (13). This suggests that binding of cAMP to cells starts at the position of LR, represented by A^H. This scheme for the activation of adenylate cyclase in *D. discoideum* is essentially identical to the activation of adenylate cyclase in vertebrates (32).

To make a model of the interactions of the B-sites that are

TABLE II

Statistical analysis of the effect of GTP and GDP on the release of bound [^{3}H]cAMP from membranes

Condition[a]	Optimal *a* value[b]	Fitted parameters[c]						
		k_{-1}			Relative abundance			
		Fast	B^S	B^{SS}	Fast	B^S	B^{SS}	Total
		$s^{-1} \times 10$	$s^{-1} \times 100$	$s^{-1} \times 1{,}000$		%		
Control								
$t = 0$ s	3	3.6 ± 0.4	4.3 ± 0.6	3.9 ± 0.9	64.1 ± 3.5	28.5 ± 0.3	7.4 ± 1.2	100.0 ± 3.7
$t = 10$ s	2		4.8 ± 0.6	3.5 ± 0.9		20.2 ± 1.4	7.1 ± 1.1	27.3 ± 1.8
+GNP, $t = 10$ s	3	2.7 ± 0.3	4.6 ± 1.2	3.7 ± 0.4	18.7 ± 1.4	4.8 ± 1.2	3.0 ± 0.1	26.5 ± 1.9
Control, $t = 120$ s	1			2.7 ± 1.1			4.6 ± 0.4	4.6 ± 0.4
+GNP, $t = 120$ s	2	2.1 ± 0.4		2.7 ± 0.6	2.8 ± 0.3		1.9 ± 0.1	4.7 ± 0.3

[a] Data from three experiments (*c.f.* Fig. 5) were combined. The conditions indicate the data points that were used for the fit. GNP indicates that GTP or GDP was added (data from GTP and GDP are combined).

[b] The fit was executed for $a = 1$–4 (number of exponentials); the *a* value with the lowest AIC value is given.

[c] The relative abundance indicates the proportioning of sites at the time-0, 10, or 120 s (see Condition) relative to total binding at $t = 0$ s.

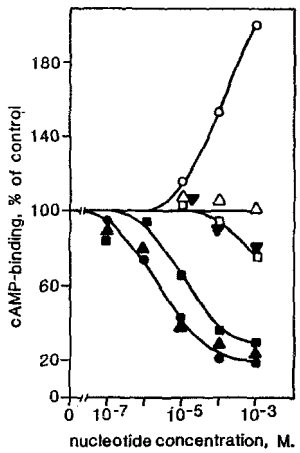

FIG. 6. **Nucleotide specificity of the alteration of [^{3}H]cAMP binding to B^S and B^{SS} in membranes from *D. discoideum*.** Membranes (derived from 10^7 cells) were incubated at 20 °C with 2 nM [^{3}H]cAMP and different concentrations of nucleotides in a volume of 100 μl for 75 s. cAMP (2 μl of 10 mM) was added, and 10 s later, membranes were centrifuged through silicon oil. The nucleotides are GTP (●), GDP (▲), GppNHp (■), GMP (▼), ATP (○), ADP (△), and AppNHp (□). Nonspecific binding was measured by including 0.1 mM cAMP in the entire incubation period; it was 155 ± 14 dpm/sample (n = 4) without the nucleotides and was changed by less than 15% in the presence of 1 mM indicated nucleotides. Specific binding was 1512 ± 52 dpm/sample (n = 3) for the control.

coupled to guanylate cyclase, we combine the general scheme with the kinetics of formation of B^S and B^{SS} in cells, with the effects of guanine nucleotides on these states in membranes, and with the observations made in desensitized cells. In membranes, the major parts of B^S and B^{SS} are converted by GTP or GDP to a fast dissociating site, indicating that LRN·GDP and LRN·GTP are fast dissociating, designated as B^F in Fig. 7*C*. In cells, the rate of formation of the B^S-state at high cAMP concentrations does not depend on the cAMP concentration, indicating that this state arises by transition from a faster dissociating state; LRN·GDP is the obvious candidate. The maximal on-rate of the B^S-state is 0.22 s^{-1}; apparently, this figure represents the transition rate constant of the step LRN·GDP → LRN. At low cAMP concentrations, the formation of the B^S-state follows Michaelis-Menten kinetics; in contrast, the formation of B^{SS} never obeys this law, but follows the kinetics of B^S. This suggests that, in the course of events, B^S is formed before B^{SS}. This view is supported by the observation that, in desensitized cells, B^S is still formed, but binding to B^{SS} is strongly reduced. The simplest explanation for these observations is that LRN is associated with B^S, and LR with B^{SS}. This would imply that activation of guanylate cyclase in *D. discoideum* is proportional to the transition of B^S to B^{SS}, a transition which no longer occurs in desensitized cells. One observation seems to be incompatible with the proposed model, *i.e.* the formation of B^{SS} in membranes. The absence of GTP would exclude the transition of B^S to B^{SS}. However, we observed that binding of [^{3}H]cAMP to B^{SS} is much slower in membranes than in cells (21). This could mean that in membranes B^{SS} is not reached via a transition of the B^S-state, but arises from direct association of cAMP to the unoccupied receptor not associated with a G-protein.

A comparison of the schemes for the activation of adenylate cyclase (Fig. 7*B*) and guanylate cyclase (Fig. 7*C*) in *D. discoideum* reveals two main differences, which could be relevant for their functioning. First, cAMP enters the A-cycle at the position of LR and the B-cycle at LRN·GDP. This difference between coupling and precoupling of receptor and G-protein could explain the effects of agents that immobilize proteins at the cell surface; these agents inhibit the cAMP-induced activation of adenylate cyclase, whereas they potentiate the activation of guanylate cyclase (40, 41). Second, the rate-limiting step in the activation of adenylate cyclase is the transition LR → LRN·GDP (Fig. 7*B*), *i.e.* the coupling of receptor with G-protein. In contrast, the rate-limiting step in the activation of guanylate cyclase is the dissociation of GDP from the LRN·GDP complex (Fig. 7*C*). This seems to be a rather unusual situation if compared to the interactions of GTP and GDP with the vertebrate G-protein (33, 42, 43). It should be noted, however, that this rate-limiting step is still very fast, showing a half-life of about 3 s. This constant is not very different from that of hormone-induced dissociation of GDP from the vertebrate G-protein (33, 44, 45). By precoupling of receptor and G-protein, less steps in the activation of a cyclase are required. This may explain why guanylate cyclase activity increases within 2 s after cAMP addition, whereas adenylate cyclase activity increases only after about 30 s.

The response induced by the ligand is proportional to the rate of passage through the cycle. The ligand may still bind to the receptor in the absence of any transition, which implies that the cell is desensitized. Indeed, this was observed in *D. discoideum* (Fig. 4). Fast (A^H, A^L, and B^F) and B^S were still occupied with cAMP in desensitized cells, but the transition of B^S to B^{SS} no longer occurred. This suggests either that GTP no longer binds to the G-protein-receptor complex in desensitized cells or that the G-protein is not activated by

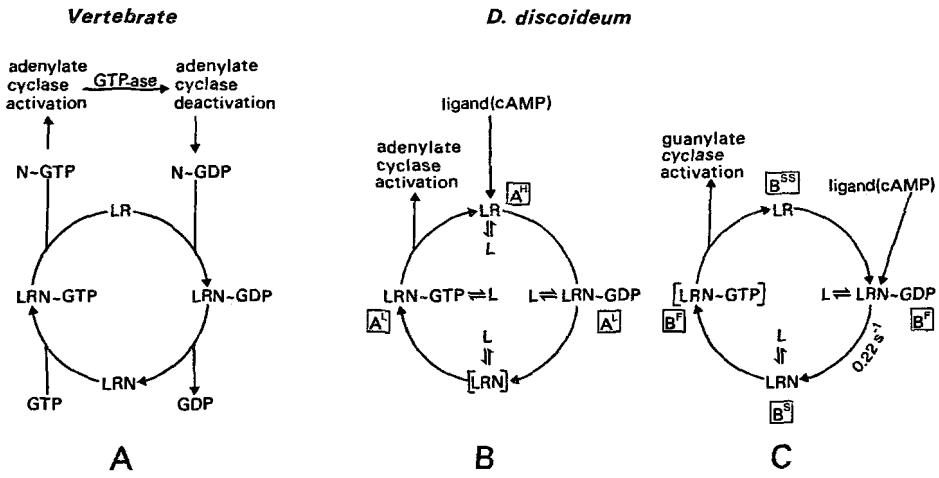

FIG. 7. **Models on the interaction between surface receptor (*R*), ligand (*L*), and guanine nucleotide-binding protein (*N*).** *A*, general scheme of hormone-induced activation of adenylate cyclase in vertebrates; *B*, scheme for the interactions of cAMP with the A-sites leading to the activation of adenylate cyclase in *D. discoideum*; *C*, scheme for the interactions of cAMP with the B-sites leading to the activation of guanylate cyclase in *D. discoideum*. See text for details.

GTP. In the former situation, the cycle would arrest in LRN (B^S), whereas in the latter case, in LRN·GTP. We observe significant amounts of LRN in cells. This would favor the former explanation.

What could be the molecular mechanism of desensitization? In vertebrates, it has been shown that phosphorylation of the receptor is associated with desensitization of the hormone-induced activation of adenylate cyclase (46–48). Phosphorylation of the receptor could be mediated by different protein kinases, including cAMP-dependent protein kinase and protein kinase C (49), and resulted in a reduced interaction of receptor and G-protein (45, 50, 51). Recently, cAMP-induced phosphorylation of the receptor has been established in *D. discoideum* (52–54) and was associated with the cAMP-induced desensitization of adenylate cyclase (55). It should be noted, however, that desensitization of guanylate cyclase is much faster than desensitization of adenylate cyclase; at 10 s after cAMP addition, guanylate cyclase is already desensitized, whereas adenylate cyclase still has to be activated (9–11). This suggests that desensitization of adenylate and guanylate cyclase does not proceed via an identical mechanism. Recently, we observed a Ca^{2+} and phorbol ester-dependent effect of ATP on the B-sites that are coupled to guanylate cyclase. The A-sites that are coupled to adenylate cyclase were not affected (30). This may indicate that the possible activation of protein kinase C in *D. discoideum* is associated with desensitization of guanylate rather than of adenylate cyclase activity. This possibility is presently being investigated.

Acknowledgments—We gratefully acknowledge Theo M. Konijn and Roel van Driel for stimulating discussions.

REFERENCES

1. Mato, J. M., and Malchow, D. (1978) *FEBS Lett.* **90,** 119–122
2. Roos, W., and Gerisch, G. (1976) *FEBS Lett.* **68,** 170–172
3. Mato, J. M., Krens, F. A., Van Haastert, P. J. M., and Konijn, T. M. (1977) *Proc. Natl. Acad. Sci. U. S. A.* **74,** 2348–2352
4. Van Haastert, P. J. M., Van Lookeren Campagne, M. M., and Ross, F. M. (1982) *FEBS Lett.* **147,** 149–152
5. Gerisch, G., and Wick, U. (1975) *Biochem. Biophys. Res. Commun.* **65,** 364–370
6. Klein, C., and Juliani, M. H. (1977) *Cell* **10,** 329–335
7. Klein, C. (1979) *J. Biol. Chem.* **254,** 12573–12578
8. Devreotes, P. N., and Steck, T. L. (1979) *J. Cell Biol.* **80,** 300–309
9. Van Haastert, P. J. M., and Van der Heijden, P. R. (1983) *J. Cell Biol.* **96,** 347–353
10. Dinauer, M. C., Steck, T. L., and Devreotes, P. N. (1980) *J. Cell Biol.* **86,** 545–553
11. Dinauer, M. C., Steck, T. L., and Devreotes, P. N. (1980) *J. Cell Biol.* **86,** 554–561
12. Pan, P., Hall, E. M., and Bonner, J. T. (1972) *Nature New Biol.* **237,** 181–182
13. Van Haastert, P. J. M., and De Wit, R. J. W. (1984) *J. Biol. Chem.* **259,** 13321–13328
14. De Wit, R. J. W., and Van Haastert, P. J. M. (1985) *Biochim. Biophys. Acta* **814,** 199–213
15. Van Haastert, P. J. M. (1985) *Biochim. Biophys. Acta* **845,** 254–260
16. Van Haastert, P. J. M. (1984) *Biochem. Biophys. Res. Commun.* **124,** 597–604
17. De Wit, R. J. W., and Bulgakov, R. (1985) *FEBS Lett.* **179,** 257–261
18. Van Haastert, P. J. M. (1985) *Biochim. Biophys. Acta* **846,** 324–333
19. Kesbeke, F., and Van Haastert, P. J. M. (1985) *Biochim. Biophys. Acta* **847,** 33–39
20. De Wit, R. J. W., Bulgakov, R., Pinas, J. E., and Konijn, T. M. (1985) *Biochim. Biophys. Acta* **814,** 214–226
21. Janssens, P. M. W., Van der Geer, P. L. J., Arents, J. C., and Van Driel, R. (1985) *Mol. Cell. Biochem.* **67,** 119–124
22. Van Haastert, P. J. M. (1983) *Biochem. Biophys. Res. Commun.* **115,** 130–136
23. Das, O. P., and Henderson, E. J. (1983) *Biochim. Biophys. Acta* **736,** 45–56
24. Pannbacker, R. G., and Bravard, J. L. (1972) *Science* **175,** 1014–1016
25. Van Haastert, P. J. M. (1981) *J. Chromatogr.* **210,** 229–240
26. Landaw, E. M., and DiStefano, J. J., III (1984) *Am. J. Physiol.* **246,** R665–R677
27. Spriet, J. A., and Vansteenkiste, G. C. (1982) *Computer-aided Modelling and Simulation*, Academic Press Inc., Ltd., London
28. Dinauer, M. C., MacKay, S. A., and Devreotes, P. N. (1980) *J. Cell Biol.* **86,** 537–544
29. Van Haastert, P. J. M. (1984) *J. Gen. Microbiol.* **130,** 2559–2564
30. Van Haastert, P. J. M., De Wit, R. J. W., and Van Lookeren Campagne, M. M. (1985) *Biochem. Biophys. Res. Commun.* **128,** 185–192
31. Cassel, D., and Selinger, Z. (1978) *Proc. Natl. Acad. Sci. U. S. A.* **75,** 4155–4159
32. Lefkowitz, R. J., Stadel, J. M., and Caron, M. G. (1983) *Annu. Rev. Biochem.* **52,** 159–186
33. Tolkowsky, A. M., Braun, S., and Levitzki, A. L. (1982) *Proc. Natl. Acad. Sci. U. S. A.* **79,** 213–217
34. Northup, J. K., Smigel, M. D., Sternweis, P. C., and Gilman, A. G. (1983) *J. Biol. Chem.* **258,** 11369–11376
35. Northup, J. K., Sternweis, P. C., and Gilman, A. G. (1983) *J. Biol. Chem.* **258,** 11361–11368
36. Hildebrandt, J. D., Codina, J., Resinger, R., and Birnbaumer, L. (1984) *J. Biol. Chem.* **259,** 2039–2042
37. Katada, T., Northup, J. K., Bokock, G. M., Ui, M., and Gilman, A. G. (1984) *J. Biol. Chem.* **259,** 3578–3585
38. Codina, J., Hildebrandt, J. D., Birnbaumer, L., and Sekura, R. D. (1984) *J. Biol. Chem.* **259,** 11408–11418
39. Brandt, D. R., and Ross, E. M. (1985) *J. Biol. Chem.* **260,** 266–272
40. Mato, J. M., Van Haastert, P. J. M., Krens, F. A., and Konijn, T. M. (1978) *Cell Biol. Int. Rep.* **2,** 163–170
41. Fontana, D. R., and Devreotes, P. N. (1984) *Dev. Biol.* **106,** 76–82
42. Northup, J. K., Smigel, M. D., and Gilman, A. G. (1982) *J. Biol. Chem.* **257,** 11416–11423
43. Birnbaumer, L., Swartz, T. L., Abramowitz, J., Mintz, P. W., and Iyengar, R. (1980) *J. Biol. Chem.* **255,** 3542–3551
44. Pike, L. J., and Lefkowitz, R. J. (1981) *J. Biol. Chem.* **256,** 2207–2212
45. Briggs, M. M., Stadel, J. M., Iyengar, R., and Lefkowitz, R. J. (1983) *Arch. Biochem. Biophys.* **224,** 142–151
46. Stadel, J. M., Nambi, P., Shorr, R. G. L., Sawyer, D. R., Caron, M. G., and Lefkowitz, R. J. (1983) *Proc. Natl. Acad. Sci. U. S. A.* **80,** 3171–3177
47. Sibley, D. R., Peters, J. R., Nambi, P., Caron, M. G., and Lefkowitz, R. J. (1984) *J. Biol. Chem.* **259,** 9742–9749
48. Kelleher, D. J., Pessin, J. E., Ruoho, A. E., and Johnson, G. (1984) *Proc. Natl. Acad. Sci. U. S. A.* **81,** 4316–4320
49. Nambi, P., Peters, J. R., Sibley, D. R., and Lefkowitz, R. J. (1985) *J. Biol. Chem.* **260,** 2165–2171
50. Kirchick, H. J., Iyengar, R., and Birnbaumer, L. (1983) *Endocrinology* **113,** 1638–1648
51. Benovic, J. L., Pike, L. J., Cerione, R. A., Staniszewski, C., Voshimasa, T., Codina, J., Caron, M. G., and Lefkowitz, R. J. (1985) *J. Biol. Chem.* **260,** 7094–7101
52. Theibert, A., Klein, P., and Devreotes, P. N. (1984) *J. Biol. Chem.* **259,** 12318–12321
53. Klein, P., Theibert, A., Fontana, D., and Devreotes, P. N. (1985) *J. Biol. Chem.* **260,** 1757–1764
54. Klein, C., Lubs-Haukeness, J., and Simons, S. (1985) *J. Cell Biol.* **100,** 715–720
55. Devreotes, P. N., and Sherring, J. A. (1985) *J. Biol. Chem.* **260,** 6378–6384